REGULARIZATION OF DIFFUSION TENSOR IMAGES

J. Cisternas[*]
Facultad de Ingeniería
Universidad de los Andes
Av. San Carlos de Apoquindo 2200
Santiago, Chile

T. Asahi
Centro de Modelamiento Matemático
Universidad de Chile
Av. Blanco Encalada 2120
Santiago, Chile

M. Gálvez, G. Rojas[†]
Instituto de Neurocirugía Dr. Asenjo
Universidad de Chile
Av. José Manuel Infante 553
Santiago, Chile

ABSTRACT

We present a regularization scheme for diffusion tensor images, that respects the geometrical structure of diffusion ellipsoids and does not introduce artifacts such as anisotropy drops.

The method can be stated as a variational problem and solved by means of a gradient flow. The main ingredient is the notion of a distance between two ellipsoids that considers differences in shape as well as differences in orientation.

The method is specialized to the case of cylindrically-symmetric ellipsoids and implemented in terms of ordinary vector manipulations such as cross and dot products.

The regularization algorithm is tested using a synthetic tensor field and a dataset acquired from a diffusion phantom. In both cases the algorithm was able to reduce the noise from the tensor field.

Index Terms— Biomedical magnetic resonance imaging, biomedical image processing, eigenvalues and eigenfunctions, smoothing methods, variational methods

1. INTRODUCTION

Diffusion Weighted Imaging (DWI) is a modality of Magnetic Resonance that measures the water molecule's diffusivity along a set of defined directions by means of the manipulation of the magnetic gradients [1]. By means of a tensor model (DTI), it is possible to describe as an ellipsoid the average distribution of movement of the water molecules within one voxel.

The principal axis of this ellipsoid will correspond to the eigevector associated to the biggest eigenvalue. For the case of the human brain tissue, this direction will correspond to the orientation of the fibers of white matter [2]. Therefore, with the information provided by DTI, we can do tractography and estimate the paths of the fibers of white matter [3].

Since the acquisition technique takes a long time, low Signal-to-Noise ratio (SNR) images are obtained. The present work is devoted to filter the noise of the images in order to present image results with less artifacts.

2. PRELIMINARIES

2.1. Tensor fields

The diffusion of water molecules in biological tissues can be effectively described using an ellipsoid that represents the average displacements produced by random forces, as depicted in Fig. 1. Such diffusion ellipsoid can be described by means of a symmetric positive-definite 3×3 matrix: the diffusion tensor. Geometrical structure of the ellipsoid, for instance its semiaxes, can be extracted from the eigenvalues and eigenvectors of the tensor.

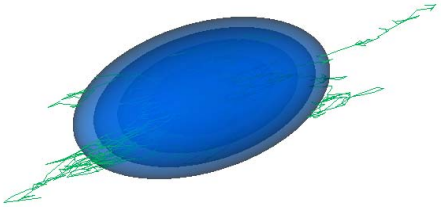

Fig. 1. The diffusion ellipsoid.

Eigenvalues λ_i of diffusion tensor D at each voxel result from the spectral decomposition:

$$D = R^T \Lambda R \,,$$

where $R \in \mathsf{SO}(3)$ corresponds to the *orientation* of the ellipsoid, and Λ, is a diagonal matrix built from the (positive) eigenvalues that corresponds to the ellipsoid *shape*:

$$\Lambda = \operatorname{diag}(\lambda_1, \lambda_2, \lambda_3) \;\;,\;\; \lambda_1 \geq \lambda_2 \geq \lambda_3 > 0 \,.$$

The estimation of the entries of the diffusion tensors is performed independently at each voxel using the Stejskal-Tanner equation [4]:

$$\log(S_i/S_0) = -b\boldsymbol{g}_i^T D \boldsymbol{g}_i \;,\; i = 1, 2, \ldots, N_{\text{dirs}} \,,$$

where S_0 is a noise-free image and $S_i (i = 1, \ldots, N_e)$ are diffusion weighted images acquired with gradient pulses along direction $\boldsymbol{g}_i \in \mathbb{R}^3$ ($|\boldsymbol{g}_i| = 1$). The factor b measures the intensity and duration of the pulsed gradients. If $N_e \geq 6$ the previous equations can be solved for the six unknowns $(D_{xx}, D_{xy}, D_{xz}, D_{yy}, D_{yz}, D_{zz})$ in the least-squares sense.

2.2. Cylindrically symmetric ellipsoids

To simplify the mathematical derivation of the regularization method, we will make the following assumption: at each voxel the diffusion has linear anisotropy $\lambda_1 \gg \lambda_2 \approx \lambda_3$. Cross-sections of ellipsoids are circular. This relation is valid in the white matter of the brain, where DTI identifies a well-defined principal direction that captures most of the diffusion.

[*]Supported by Fondecyt Grant 1070098.
[†]Supported by Fondecyt Grant 1070550.

Then we can write the diffusion tensor using a single orientation $\boldsymbol{u}$ and two diffusivities; one longitudinal $\lambda_\parallel$ and other transversal $\lambda_\perp$:

$$D = (\lambda_\parallel - \lambda_\perp)\boldsymbol{u}\boldsymbol{u}^T + \lambda_\perp Id \; .$$

The vector $\boldsymbol{u}$ takes values on the surface of a unitary sphere S^2 where antipodal points $\boldsymbol{u}$ and $-\boldsymbol{u}$ are identified, as shown in Fig. 2.

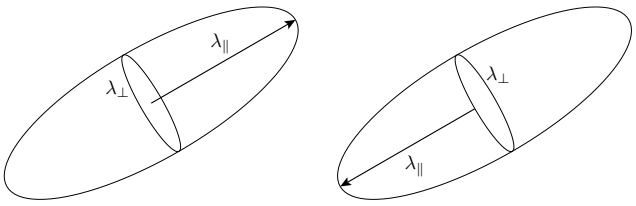

Fig. 2. Cylindrically-symmetric ellipsoids

2.3. Regularization of diffusion weighted images

A first approach to denoising would be to process the grayscale images S_i, before the estimation of tensors, using standard filtering schemes.

2.3.1. Total Variation

We consider the model of Total Variation, developed by Rudin, Osher, and Fatemi [5], that reduces the noise but preserves rapid and isolated variations. This feauture should in principle minimize partial-volume artifacts that are created when signals coming from different tissues, for instance white matter and cerebro-spinal fluid, are mixed.

The model is based on a functional TV that results from adding local variations between each voxel and its neighbors (here we use a three dimensional neighborhood of 6 voxels). Using notation borrowed from graph theory (after [6]):

$$TV[S] \stackrel{\text{def}}{=} \sum_{\alpha\in\Omega} \left(\sum_{\beta\in\omega_\alpha} w_{\alpha,\beta} \left(S_\alpha - S_\beta\right)^2 \right)^{1/2} \; ,$$

where Ω is the whole 3-D domain of the signal S, ω_α is the set of neighbors of voxel α, and $w_{\alpha,\beta}$ is a positive weight that depends on the distance between each pair of neighbors.

To define a well-posed minimization problem, one must keep S close from the noisy signal $S^{(0)}$. The voxel-wise difference defines a fidelity functional:

$$F[S, S^{(0)}] \stackrel{\text{def}}{=} \sum_{\alpha\in\Omega} (S_\alpha - S^{(0)}_\alpha)^2 \; .$$

We could minimize $TV[S]$ imposing a given value for $F[S, S^{(0)}]$, or the other way around. This could be better framed introducing a positive Lagrange multiplier η:

$$J[S, S^{(0)}] \stackrel{\text{def}}{=} TV[S] + \frac{\eta}{2} F[S, S^{(0)}] \; .$$

Minimizing $J[\cdot]$ using a large value of parameter η gives images with mild smoothing, using a small value of η gives a smooth image with little similarity to the original. Appropriate values for parameter η depend on the specific application and the scale of values of image $S^{(0)}$.

A general and efficient minimization scheme that continuously transforms a given image $S^{(0)}$ into a regularized version can be obtained considering a gradient flow.

It can be proved that for a $S(t)$ that satisfies the ODE:

$$\frac{\mathrm{d}S_\alpha}{\mathrm{d}t} = \sum_{\beta\in\omega_\alpha} \left(\frac{1}{e_\alpha} + \frac{1}{e_\beta} \right) w_{\alpha,\beta}(S_\beta - S_\alpha) + \eta(S^{(0)}_\alpha - S_\alpha) \; ,$$

where the local variation $e_\alpha = \sqrt{\sum_{\beta\in\omega_\alpha}(S_\beta - S_\alpha)^2}$, the value of $J[S(t), S^{(0)}]$ does not increase and will converge in general.

2.3.2. Multi-channel Total Variation

One could also process the whole dataset $S_i (i = 0, \ldots, N_e)$ (N_e diffusion weighted images and one diffusion-free image) at the same time. Following [7], we define the distance between two voxels:

$$d(S_\alpha, S_\beta) \stackrel{\text{def}}{=} \left(\sum_{i=0}^{N_e} (S_{\alpha,i} - S_{\beta,i})^2 \right)^{1/2} \; ,$$

and we would get for each channel i:

$$\frac{\mathrm{d}S_{\alpha,i}}{\mathrm{d}t} = \sum_{\beta\in\omega_\alpha} \left(\frac{1}{e_\alpha} + \frac{1}{e_\beta} \right) w_{\alpha,\beta}(S_{\beta,i} - S_{\alpha,i}) + \eta(S^{(0)}_{\alpha,i} - S_{\alpha,i}) \; ,$$

where the local variation:

$$e_\alpha \stackrel{\text{def}}{=} \left(\sum_{i=0}^{N_e} \sum_{\beta\in\omega_\alpha} (S_{\alpha,i} - S_{\beta,i})^2 \right)^{1/2}$$

effectively *couples* all the channels. As the flow progresses, edges in one channel affect the smoothing in all other channels.

A similar multi-channel approach could be applied after the estimation of the diffusion tensors D, regularizing the entries $D_{xx}, D_{yy}, D_{zz}, D_{xy}, D_{xz}, D_{yz}$, either separately or coupled. Other approaches have considered the regularization of some factorization of D (see for instance [8, 9]).

But all the previously described methods suffer from the same limitation: the regularization makes ellipsoids more spherical. This artefact is referred as 'ellipsoid swelling' (see Fig. 3) and can be recognized as a loss of anisotropy. By linearly combining neighboring tensors that are not perfectly aligned, more spherical ellipsoids are created.

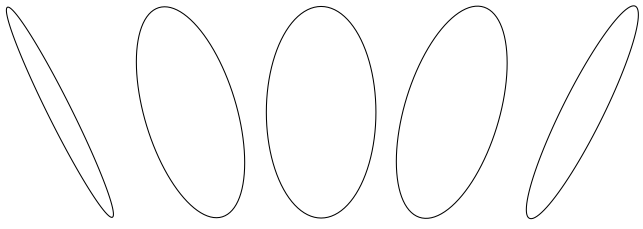

Fig. 3. Ellipsoid swelling

3. REGULARIZATION OF TENSORS

A number of regularization approaches for DTI have been proposed to reduce the noise and overcome the swelling, most notably [10, 11]. Here we build on previous works but choose to keep the geometrical concepts as clear as possible, using measures of distance between two ellipsoids inspired in rotations.

For cylindrically-symmetric ellipsoids, we define a distance by considering differences in orientation and shape:

$$d^2(D_\alpha, D_\beta) \stackrel{\text{def}}{=} d^2_{\text{or}}(\boldsymbol{u}_\alpha, \boldsymbol{u}_\beta) + s_\parallel(\lambda_{\parallel,\alpha} - \lambda_{\parallel,\beta})^2 + s_\perp(\lambda_{\perp,\alpha} - \lambda_{\perp,\beta})^2 , \quad (1)$$

where $s_\parallel, s_\perp$ are two positive weights. For the distance between two orientations we take the *sharp* angle:

$$d_{\text{or}}(\boldsymbol{u}_\alpha, \boldsymbol{u}_\beta) = \arcsin(||\boldsymbol{u}_1 \times \boldsymbol{u}_2||) \in \left[0, \frac{\pi}{2}\right] . \quad (2)$$

If $\boldsymbol{u}_1, \boldsymbol{u}_2$ are parallel then $d_{\text{or}}(\boldsymbol{u}_1, \boldsymbol{u}_2) = 0$. This definition is the geodesic distance and also satisfies:

$$d_{\text{or}}(\boldsymbol{u}_1, \boldsymbol{u}_2) = d_{\text{or}}(-\boldsymbol{u}_1, \boldsymbol{u}_2) = d_{\text{or}}(\boldsymbol{u}_2, \boldsymbol{u}_1) .$$

We then define a functional that includes local variations of neighboring ellipsoids:

$$TV[D] \stackrel{\text{def}}{=} \sum_{\alpha\in\Omega} e_\alpha(D_\alpha) \ , \ e_\alpha \stackrel{\text{def}}{=} \left(\sum_{\beta\in\omega_\alpha} w_{\alpha,\beta}\, d^2(D_\alpha, D_\beta) \right)^{1/2} , \quad (3)$$

and a functional that measures the distance to the original tensor field $D^{(0)}$:

$$F[D, D^{(0)}] \stackrel{\text{def}}{=} \sum_{\alpha\in\Omega} d^2(D_\alpha, D^{(0)}_\alpha) , \quad (4)$$

where Ω is the set of voxels with linear anisotropy, and ω_α is the set of neighbors of α.

As before, we introduce a positive multiplier η and pose the following variational principle:

$$J[D, D^{(0)}] \stackrel{\text{def}}{=} TV[D] + \frac{\eta}{2} F[D, D^{(0)}] . \quad (5)$$

Using $\boldsymbol{v}_{\alpha,\beta} = \theta\boldsymbol{e}$, where θ is the angle and $\boldsymbol{e}$ is the axis of the rotation that transforms $\boldsymbol{u}_\alpha$ into $\boldsymbol{u}_\beta$, it can be shown that the gradient flow can be written in the form of the following three differential equations:

$$\frac{\mathrm{d}\boldsymbol{u}_\alpha}{\mathrm{d}t} = \Big(\sum_{\beta\in\omega_\alpha} \left(\frac{1}{e_\alpha} + \frac{1}{e_\beta}\right) w_{\alpha,\beta}\boldsymbol{v}_{\alpha,\beta} + \eta\, \boldsymbol{v}_{\alpha,\alpha^{(0)}} \Big) \times \boldsymbol{u}_\alpha , \quad (6)$$

$$\frac{\mathrm{d}\lambda_{\parallel,\alpha}}{\mathrm{d}t} = \sum_{\beta\in\omega_\alpha} \left(\frac{1}{e_\alpha} + \frac{1}{e_\beta}\right) w_{\alpha,\beta}(\lambda_{\parallel,\beta} - \lambda_{\parallel,\alpha}) + \eta(\lambda^{(0)}_{\parallel,\alpha} - \lambda_{\parallel,\alpha}) , \quad (7)$$

$$\frac{\mathrm{d}\lambda_{\perp,\alpha}}{\mathrm{d}t} = \sum_{\beta\in\omega_\alpha} \left(\frac{1}{e_\alpha} + \frac{1}{e_\beta}\right) w_{\alpha,\beta}(\lambda_{\perp,\beta} - \lambda_{\perp,\alpha}) + \eta(\lambda^{(0)}_{\perp,\alpha} - \lambda_{\perp,\alpha}) , \quad (8)$$

plus some appropriate initial conditions. As with the multi-channel regularization presented in Section 2.3.2, the flow defined by Eqns. (6–8) makes the value of the functional $J[\cdot]$ to decrease and couples the smoothing of orientations and shapes.

Efficient iterative implementation of the gradient flow relies on the Rodrigues' formula for the rotation of orientations [11]. There is no need of projecting or normalizing the orientations. After the flow converges, the diffusion tensor field D can be reconstructed from $\boldsymbol{u}, \lambda_\parallel, \lambda_\perp$. Regularization of tensor fields should improve the results of tractography algorithms that track likely trajectories of neural fibers but break down after reaching voxels of low anisotropy or highly incoherent orientations.

4. EVALUATION

For the testing of the proposed algorithm we used two examples of tensor fields.

4.1. Synthetic tensor field

The first example is a synthetic tensor field taken from Ref. [8]. It is a $50 \times 50 \times 5$ volume, where initially each one of the five horizontal slices was divided into four quadrants, with the following orientations $\boldsymbol{u} = (0, 1, 0)$, $\boldsymbol{u} = (1, 1, 0)/\sqrt{2}$, $\boldsymbol{u} = (1, -1, 0)/\sqrt{2}$, and $\boldsymbol{u} = (0, 0, 0)$. The bottom-left quadrant was left without a coherent orientation. Tensors D were built using $\lambda_\parallel = 1, \lambda_\perp = 1/3$ everywhere. Gaussian noise (0 mean, 0.2 standard deviation) was added to each component of the tensor D (preserving its symmetry). After tensors were diagonalized, the regularization algorithm was applied to the noisy $\boldsymbol{u}, \lambda_\parallel, \lambda_\perp$ fields.

Results are shown using the RGB colorcode: red means $|u_x|$ orientation, green means $|u_y|$, and blue means $|u_z|$. Intensity is modulated by anisotropy: bright color means $\lambda_\perp \ll \lambda_\parallel$, dark color means $\lambda_\parallel \approx \lambda_\perp$. A single slice is shown in Fig. 4, (a) before, and (b) after the regularization. Please notice that the color code is ambiguous; orange represents both $(1, -1, 0)$ and $(1, 1, 0)$ orientations, which are actually perpendicular.

The algorithm was able to reconstruct the right orientation in each of the four quadrants, preserving a clear boundary between them and removing noisy spots. The algorithm did not create a spurious orientation in the bottom-left quadrant.

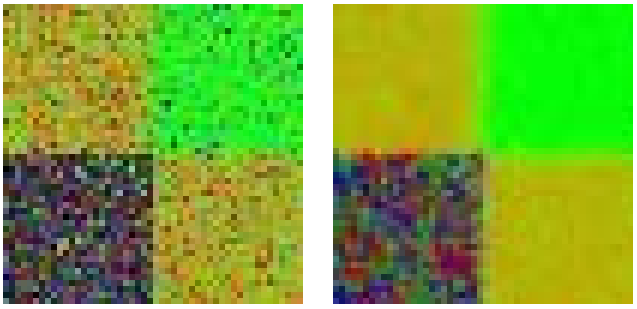

(a) (b)

Fig. 4. Regularization of a synthetic tensor field

4.2. Diffusion phantom

For a more realistic test we used a phantom provided by the Radiology Department of the Deutsches Krebsforschungszentrum (DKFZ) and described in Ref. [12]. The phantom consists of a single polyfil

polyamid fiber (diameter 50 μm) which was wound $30,000$ times around an acrylic spindle, as shown in Fig. 5. This fiber has similar diffusion and relaxation properties than those of white matter, and verifies the linear anisotropy assumption used in this work and explained in Section 2.2. The phantom was put into a water bath and its diffusion weighted images were acquired using a Philips Intera 1.5T scanner ($b = 800\,\mathrm{s/cm^2}$, 6 directions, 10 averages, voxel size $= 1.75 \times 1.75 \times 2.5\,\mathrm{mm^3}$). Only two slices (perpendicular to the axis of the spindle) were processed.

Fig. 5. Polyamid fiber phantom

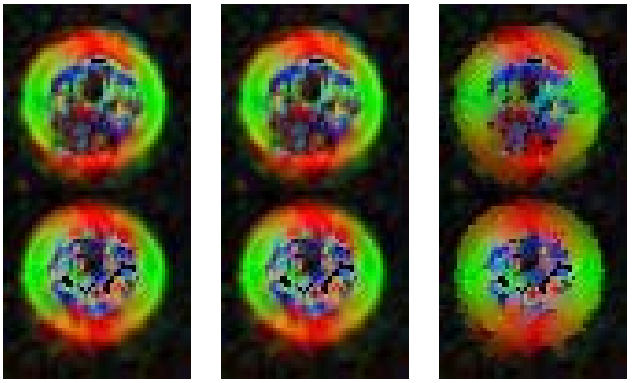

$\eta = 20$ $\eta = 10$ $\eta = 0$

Fig. 6. Regularization of a phantom tensor field

In Fig. 6 results are presented for three values of the multiplier η. As smaller values of the multiplier are used, smoothing is performed more aggressively. Notice that, opposite from regularization of gray-scale images, using $\eta = 0$ does not lead to homogeneous fields. The intrinsic curvature of the space of ellipsoids creates many local minima where the gradient flow converges. These minima preserve some properties of the reference field $D^{(0)}$. Looking attentively Fig. 6, one could appreciate that between $\eta = 20$ and $\eta = 10$ there are only some minor changes in intensity (shape) and color (orientation).

Preliminary results indicate that best results are obtained when the following sequence of steps is used: (1) regularization of DWI dataset using multi-channel method, (2) estimation of DTI, and (3) regularization of DTI with proposed model.

The impact of local minima could be reduced by a multi-resolution scheme built on top of the present regularization algorithm. The whole approach can be generalized to diffusion tensors of any shape, defining a distance between two tensors (see Eqn. (1)) that includes six terms: the three angles between the corresponding pairs of eigenvectors, and the three differences between the corresponding pairs of eigenvalues.

5. CONCLUSIONS

The present tensor field regularization framework extends the notion of distance to the orientation and shape of axially-symmetric tensors. Using a gradient flow built from a variational principle, we were able to reduce the noise of DTI datasets and increase the directional homogeneity of fiber bundles of a phantom. The proposed method can potentially improve results of tractography in regions of high SNR. The approach can be extended to non-degenerate ellipsoids, defining a distance that takes into account the second and third eigenvectors and eigenvalues.

6. REFERENCES

[1] P.J. Basser, J. Mattiello, and D. Le Bihan, "Estimation of the effective self-diffusion tensor from the NMR spin echo," *J. Magn. Reson. B*, vol. 103, pp. 247–254, 1994.

[2] C. Beaulieu, "The basis of anisotropic water diffusion in the nervous system — a technical review," *NMR Biomed.*, vol. 15, pp. 435–455, 2002.

[3] T.E. Conturo, N.F. Lori, T.S. Cull, E. Akbudak, A.Z. Snyder, J.S. Shimony, R.C. McKinstry, H. Burton, and M.E. Raichle, "Tracking neuronal fiber pathways in the living human brain," *Proc. Natl. Acad. Sci. USA*, vol. 96, pp. 10422–10427, 1999.

[4] E.O. Stejskal and J.E. Tanner, "Spin diffusion measurements: spin echoes in the presence of a time-dependent field gradient," *J. Chem. Phys.*, vol. 42, pp. 288–292, 1965.

[5] L. Rudin, S. Osher, and E. Fatemi, "Nonlinear total variation based noise removal algorithms," *Physica D*, vol. 60, pp. 259–268, 1992.

[6] T.F. Chan, S. Osher, and J. Shen, "The digital TV filter and nonlinear denoising," *IEEE Transactions on Image Processing*, vol. 10, no. 2, pp. 231–241, 2001.

[7] G. Sapiro and D. L. Ringach, "Anisotropic diffusion of multivalued images with applications to color filtering," *IEEE Transactions on Image Processing*, vol. 5, no. 11, pp. 1582–1586, 1996.

[8] O. Christiansen, J. Lie T. Lee, U. Sinha, and T. Chan, "Total Variation regularization of matrix-valued images," *International Journal of Biomedical Imaging*, pp. 1–11, 2007.

[9] D. Tshumperlé and R. Deriche, "Variational frameworks for DT-MRI estimation, regularization and visualization," in *Ninth IEEE International Conference on Computer Vision*, 2003.

[10] O. Coulon, D.C. Alexander, and S. Arridge, "Diffusion tensor magnetic resonance image regularization," *Medical Image Analysis*, vol. 8, pp. 47–67, 2004.

[11] C. Chefdhotel, D. Tschumperlé, R. Deriche, and O. Faugeras, "Regularizing flows for constrained matrix-valued images," *Journal of Mathematical Imaging and Vision*, vol. 20, no. 1–2, pp. 147–162, 2004.

[12] F.B. Laun, B. Stieltjes, S. Huff, and L.R. Schad, "Investigation of a DTI-phantom with properties similar to *in vivo* neuronal tissue," in *Proc. Intl. Mag. Reson. Med.*, Berlin, 2007, vol. 15, p. 1526.